J. Fluid Mech. (2003), *vol.* 478, *pp.* 81–100.
DOI: 10.1017/S0022112002003269 Printed in the United Kingdom

Shoaling solitary internal waves: on a criterion for the formation of waves with trapped cores

By KEVIN G. LAMB

Department of Applied Mathematics, University of Waterloo, Waterloo, Ontario, Canada N2L 3G1

(Received 11 February 2002 and in revised form 25 September 2002)

Shoaling solitary internal waves are ubiquitous features in the coastal regions of the world's oceans where waves with a core of recirculating fluid (trapped cores) can provide an effective transport mechanism. Here, numerical evidence is presented which suggests that there is a close connection between the limiting behaviour of large-amplitude solitary waves and the formation of such waves via shoaling. For some background states, large-amplitude waves are broad, having a nearly horizontal flow in their centre. The flow in the centre of such waves is called a conjugate flow. For other background states, large-amplitude waves can reach the breaking limit, at which the maximum current in the wave is equal to the wave's propagation speed. The presence of a background current with near-surface vorticity of the same sign as that induced by the wave can change the limiting behaviour from the conjugate-flow limit to the breaking limit. Numerical evidence is presented here which suggests that if large solitary waves cannot reach the breaking limit in the shallow water, that is if the background flow has a conjugate flow, then waves with trapped cores will not be formed via shoaling. It is also shown that, due to a change in the limiting behaviour of large waves, an appropriate background current can enable the formation of waves with trapped cores in stratifications for which such waves are not formed in the absence of a background current.

1. Introduction

Shoaling internal solitary waves (ISWs) are common in coastal regions of the world's oceans where waves with trapped cores can provide a very effective mechanism for the transport of fluid. Hence, it is of interest to determine the conditions under which such waves can be formed. In an earlier investigation of shoaling ISWs, Lamb (2002) focused on stratifications which monotonically increased in strength towards the surface. No background currents were present. It was found that sufficiently large deep-water solitary waves formed waves with trapped cores in the shallow water. Grue *et al.* (2000) performed laboratory experiments using a continuous monotonic stratification consisting of a layer of fluid with constant buoyancy frequency overlying a homogeneous layer. They reported the formation of waves with maximum velocities exceeding the wave propagation speed. This suggests the presence of a trapped core, although waves may not have reached a final steady state. Solitary internal waves with trapped cores have been observed in the ocean off the coast of oregon under conditions with stratification close to the surface (D. Farmer, personal communication).

In his numerical simulations of shoaling waves, Lamb (2002) modified an exponential stratification by adding a thin surface mixed layer and found that waves with trapped cores were no longer formed. He suggested that the inhibition of the

formation of waves with trapped cores by the surface mixed layer is associated with a change in the limiting behaviour of large-amplitude solitary waves. In the presence of the surface mixed layer, the shallow-water stratification has a non-breaking conjugate flow of depression. That is, large solitary waves in shallow water become horizontally uniform in their centre. As the energy in the wave increases waves become longer, while the wave amplitude, maximum horizontal velocity $U_{\max}$ and wave propagation speed c asymptote to constant values with $U_{\max}/c < 1$. If this occurs ISWs are said to conjugate-flow limited. In contrast, for the monotonic stratifications, which were the focus of the paper, amplitudes of solitary waves with open streaklines (streamlines in a reference frame moving with the wave) are limited by the breaking limit at which $U_{\max}/c = 1$.

The reason for the significant difference in the limiting behaviour of large waves for the exponential stratification with and without a surface mixed layer is that in the mixed layer there is no mechanism for the generation of vorticity. In the centre of a large solitary wave of depression the surface mixed layer is stretched in the vertical, resulting in a much thicker layer of low vorticity. Hence the presence of a thin surface mixed layer can significantly modify the near-surface velocity field in a large solitary wave of depression. In particular, the near-surface velocity, and hence $U_{\max}$, at the centre of the solitary wave is significantly reduced. This results in waves in the mixed layer stratification being conjugate-flow limited whereas for the exponential stratification, solitary waves could reach the breaking limit. This explanation for the change in limiting behaviour also suggests that the limiting behaviour of large-amplitude ISWs of depression is sensitive to the presence of near-surface vorticity in the background flow.

Here, numerical evidence is presented which is consistent with the hypothesis that waves with trapped cores cannot be formed if a conjugate flow with open streaklines exists. Only waves of depression are considered. Such evidence is provided for a family of stratifications with and without a background current. It is also shown that the presence of a background sheared current, with near-surface vorticity of the same sign as the wave-induced vorticity, can enable the formation of waves with trapped cores in a stratification that cannot support such waves in the absence of a background current. This change in the shoaling behaviour is believed to be a consequence of the fact that the background current changes the limiting behaviour of large ISWs with open streaklines from the conjugate flow limit to the breaking limit.

The plan of the paper is as follows. In § 2 the equations of motion are presented in nondimensional form and the numerical models and the model stratifications and background currents used are described. In § 3 the effects of background currents on the existence of conjugate flows is investigated, as this is the criterion relevant to the formation of waves with cores. Section 4 presents the results of the numerical simulations of shoaling waves. A summary is given in § 5.

2. Governing equations and the numerical model

A schematic of the model setup indicating the meaning of the key parameters used for the topography, stratification and background velocity is given in figure 1.

The model equations used in this study are the incompressible Euler equations under the Boussinesq approximation, whereby in the momentum equation the density is replaced by a constant representative value ρ_0 except when multiplied by g^*, the gravitational acceleration. The equations are non-dimensionalized using the shallow-water depth D as the length scale, the shallow-water, mode-1, linear long-wave

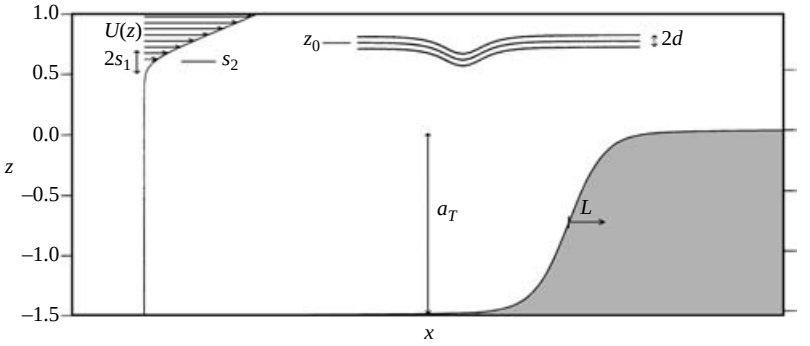

FIGURE 1. Schematic of the model setup. The model is initialized with a single internal solitary wave in the deep water which propagates to the right into shallower water. In the background current $U(z)$ the vorticity changes to a constant value at $z = s_2$ over a distance of $2s_1$. The pycnocline is centred at z_0 and has a thickness of $2d$. The shelf amplitude has amplitude a_T (equal to 1.5 in this figure) and half-width L.

propagation speed $\bar{U} = \bar{N}D/\pi = \sqrt{g^*\delta\rho D}/\pi$ as the velocity scale, and the advective time scale $D/\bar{U}$. Here $\rho_0\delta\rho$ is representative of the density change over the water column and $\bar{U}$ would be the propagation speed if the undisturbed density varied linearly. Thus, using standard terminology and starred/unstarred variables to represent the dimensional/non-dimensional variables, we set

$$(x^*, z^*) = D(x, z), \quad (u^*, W^*) = \bar{U}(u, w), \quad t^* = \frac{D}{\bar{U}}t, \tag{1a}$$

$$\rho^* = \rho_0(1 + \delta\rho\rho), \quad p^* = \rho_0(-g^*z^* + \bar{U}^1 p). \tag{1b}$$

The non-dimensional governing equations are then

$$\boldsymbol{U}_t + \boldsymbol{U}\cdot\nabla\boldsymbol{U} = -\nabla p - \rho\pi^2\hat{\boldsymbol{k}}, \tag{2a}$$

$$\rho_t + \boldsymbol{U}\cdot\nabla\rho = 0, \tag{2b}$$

$$\nabla\cdot\boldsymbol{U} = 0. \tag{2c}$$

The rigid-lid approximation is made which removes surface waves from the problem. The surface is at $z = 1$ and the bottom is at

$$z = h(x) = -\frac{a_T}{2}\left(1 - \tanh\left(\frac{x}{L}\right)\right), \tag{3}$$

where a_T and L are positive parameters determining the shelf amplitude and shelf width. The total water depth $1 - h(x)$ decreases monotonically from $1 + a_T$ in the deep water for $x \ll -L$ to the shallow-water depth of 1 for $x \gg L$.

For the undisturbed density field, stratifications consisting of a single pycnocline, given by the two-parameter family

$$\bar{\rho}(z) = -0.5\tanh\left(\frac{z - z_0}{d}\right), \tag{4}$$

are used.

As discussed in the introduction, it seems reasonable that a background flow with near-surface vorticity of the same sign as that generated in the solitary wave by baroclinicity can result in breaking waves for stratifications that would have

conjugate-flow-limited waves in the absence of such a current. We explore this idea by considering the effects of a background current with near-surface vorticity. In order to avoid the complication of wave generation by the background current as it flows over the shelf slope, a surface-trapped background current is used. It has the form

$$U(z) = \frac{\zeta}{2}\left(z - s_2 + s_1 \ln\left(\cosh\left(\frac{z - s_2}{s_1}\right)\right)\right), \tag{5}$$

which has vorticity

$$U'(z) = \frac{\zeta}{2}\left(1 + \tanh\left(\frac{z - s_2}{s_1}\right)\right). \tag{6}$$

The background velocity is zero for large $-z$, undergoing a smooth transition to a constant sheared flow at $z = s_2$. The value of $s_1 > 0$ determines the width of the transition region. Values of s_1 and s_2 are chosen to ensure that $U(z)$ is negligibly small near and below the top of the shelf at $z = 0$. In the ocean solitary internal waves are predominantly generated by tidal flow over topographic features. We ignore such currents as the goal here is to understand the conditions under which waves with trapped cores may exist.

The numerical model used to solve (2*a–c*) is the terrain-following coordinate model described in Lamb (1994, 2002). Rotation is not included for these simulations. All model runs use evenly spaced grid points in the horizontal with a grid spacing δx. There are J grid points in the vertical. Usually $J = 120$ but a few runs with $J = 150$ and 200 were made for some marginal cases. In the shallow water a variable vertical grid spacing δz has been used, with δz decreasing quadratically towards the surface in the shallow water. This provides higher resolution in regions where wave breaking occurs. In the shallow water the vertical resolution is about 0.01325 at the bottom and 0.0034 at the surface when $J = 120$. In the deep-water region, where the initial wave is added, δz is vertically uniform.

The model is initialized with a single ISW. In a reference frame moving with the ISW the flow is steady and the equations of motion can be written as†

$$\nabla^2\eta + \frac{U'(z-\eta)}{c - U(z-\eta)}\left(\eta_x^2 + (1-\eta_z)^2 - 1\right) + \frac{N^2(z-\eta)}{(c - U(z-\eta))^2}\eta = 0. \tag{7}$$

This is the well-known Dubreil–Jacotin–Long (DJL) equation written in terms of $\eta(x, z)$, the vertical displacement of the streamline passing through (x, z) relative to its far-upstream height. Here c is the unknown wave propagation speed and

$$N^2(z) = -\pi^2\bar{\rho}'(z) \tag{8}$$

is the square of the buoyancy frequency outside the wave. For the simulations of shoaling solitary waves the initial wave is in the deep water. The boundary conditions appropriate for a solitary wave are

$$\eta = 0 \quad \text{at} \quad z = -a_T, 1 \quad \text{and} \quad \eta \to 0 \quad \text{as} \quad x \to \pm\infty. \tag{9}$$

To calculate an ISW numerically, it is approximated by setting $\eta = 0$ at $x = x_0 \pm R$ where x_0 is the position of the wave and R is large compared with the wave width. Equation (7) is solved using a method based on the variational technique developed by Turkington, Eydeland & Wang (1992) which has been generalized to include

† If the Boussinesq approximation is not made the coefficient of the second term becomes $U'(z-\eta)/(c - U(z-\eta)) + N^2(z-\eta)/2\pi^2$.

a specified background current (Stastna & Lamb 2002). The wave amplitude is determined by specifying the available potential energy (APE) of the solitary wave. Other authors investigating ISWs have used different techniques to solve the DJL equation (Davis & Acrivos 1967; Tung, Chan & Kubota 1982; Brown & Christie 1998; Grue *et al.* 2000) in the absence of a background current. Several authors have also calculated fully nonlinear solitary waves in two-layer fluids and investigated the limiting forms for such waves (Mehrotra & Kelly 1973; Holyer 1979; Saffman & Yuen 1982; Amick & Turner 1986; Turner & Vanden-Broeck 1986; Grue *et al.* 1997, 1999). In the Boussinesq limit, broad waves with a conjugate flow are formed in fluids of finite depth. Melville & Helfrich (1987) have shown how such waves may be generated by a time-varying transcritical flow over a bump. They used the forced extended KdV equation in the context of a two-layer fluid. The same evolution equation arises for continuous stratifications, hence qualitatively similar results are expected for at least those stratifications for which the weakly nonlinear theory is valid. When the Boussinesq approximation is not made and the two layers have large density differences, waves past the breaking limit ($U_{\max} = c$) can be formed which have overhangs (Holyer 1979; Saffman & Yuen 1982; Amick & Turner 1986; Turner & Vanden-Broeck 1986, 1988).

Once η and c are known the density and velocity fields are given by

$$\rho(x, z) = \bar{\rho}(z - \eta(x, z)), \tag{10}$$

and

$$(u, w) = (c - U(z - \eta))\,(\eta_z - 1, -\eta_x). \tag{11}$$

Here, u is the total horizontal velocity in the reference frame moving with the wave. The wave-induced horizontal velocity u_w is obtained by subtracting the background flow $U(z) - c$.

The wave amplitude, $\eta_{\max}$, is defined as the magnitude of the maximum isopycnal displacement. Waves with open streaklines are limited in amplitude in one of three ways (Lamb 2002). Two of these, the breaking limit and the conjugate-flow limit, were discussed in the introduction. Waves can become unstable before either of these limits are reached, giving the third amplitude limitation. For a more complete discussion see Lamb (2002).

The horizontally uniform flow in the centre of long flat waves is called a conjugate flow (Benjamin 1966; Mehrotra & Kelly 1973; Lamb & Wan 1998). In the centre of a flat-centred wave η becomes independent of x. Equation (7) then reduces to (Lamb 2000)

$$\eta'' + \frac{U'(z - \eta)}{c - \bar{U}(z - \eta)}\eta'(\eta' - 2) + \frac{N^2(z - \eta)}{(c - \bar{U}(z - \eta))^2}\eta = 0. \tag{12}$$

We will be concerned with the existence of conjugate flows in the shallow water where the boundary conditions are

$$\eta(0) = \eta(1) = 0. \tag{13}$$

Due to the nonlinearity of the eigenvalue problem (12)–(13), an auxiliary condition is required to determine $\eta'(0)$. This is obtained from consideration of conservation of momentum (Benjamin 1966; Lamb & Wan 1998), which requires that

$$M = \int_0^1 (p + u^2)\,\mathrm{d}z \tag{14}$$

is independent of x in a reference frame moving with the wave. For our application, a comparison of the flow field in the conjugate flow and the flow field outside the wave results in the auxiliary condition

$$T(\eta'(0)) = \int_0^1 (c - U(z - \eta(z)))^2 \, \eta'^3(z) \, \mathrm{d}z = 0. \tag{15}$$

Thus, $\eta'(0)$ must be chosen so that this condition is satisfied. If the Boussinesq approximation is not made then an additional factor of $(1 + \delta\rho \, \rho(z - \eta))$ is needed in the integrand (Lamb 2000). The solution of (12), (13) and (15) is a valid conjugate flow solution unless $\eta'(z) > 1$ anywhere, in which case the solution is discarded. This condition is necessary to guarantee that all streaklines extend to $\pm\infty$, an assumption used to derive (7) and (15). If a solution with $\eta'(z) \leqslant 1$ cannot be found then the upstream flow profile $\bar{\rho}(z)$ does not have a conjugate flow with open streaklines.

The nonlinear eigenvalue problem (12), coupled with the auxiliary condition (15), can have multiple mode-1 solutions. As many as three mode-1 conjugate flows have been found for some stratifications, only two of which seem to correspond to limiting solitary wave amplitudes (Lamb & Wan 1998). As will be shown, for the stratifications considered here, for sufficiently wide pycnoclines there can be three conjugate flow solutions in the presence of strong background vorticity.

3. Effect of background currents on the existence of conjugate flows

Here we explore how the existence of conjugate flows is affected by background currents of the form (5). A non-dimensional depth of 1 is used with $z = 0$ at the bottom.

Lamb & Wan (1998) investigated conjugate flows for stratifications of the form (4) in the absence of a background current. They showed that conjugate flows with open streaklines exist only when the centre of the pycnocline is greater than a critical distance $r(d)$ from the upper or lower boundary. This can be understood in the following way. For thin pycnoclines with a small density change (i.e. the Boussinesq approximation is applicable), the centre of the pycnocline is always close to the mid-depth in the conjugate flow (Lamb & Wan 1998). It is exactly at the mid-depth for a two-layer fluid (Amick & Turner 1986; Lamb 2000). Thus, as the undisturbed pycnocline moves away from the mid-depth towards a boundary, the larger the displacement in the conjugate flow becomes. The velocity jump across the pycnocline increases more rapidly than the propagation speed of the front does. For a pycnocline of finite thickness the point is reached when the conjugate flow breaks ($\max \eta'(z) = 1$). The distance from the boundary at which the conjugate flow breaks down, $r(d)$, decreases monotonically to zero as the pycnocline thickness d decreases to zero.

For a fixed background current of the form (5), two curves can be found numerically along which conjugate flows are at the breaking limit. Along $z_0 = r_l(d)$, conjugate flows of elevation are at the breaking limit (i.e. $\max \eta'(z) = 1$), while along $z_0 = r_u(d)$ conjugate flows of depression are at the breaking limit. Usually, $r_l(d) < r_u(d)$ and conjugate flows exist only if $r_l(d) < z_0 < r_u(d)$, i.e. only if the pycnocline is sufficiently far from the boundary. When there is no background current $r_u(d) = 1 - r_l(d)$ and $r_l(d)$ is always less than $r_u(d)$. It has been found, however, that for sufficiently strong background vorticity the curves $z_0 = r_l(d)$ and $z_0 = r_u(d)$ cross once so that $r_u(d) < r_l(d)$ for sufficiently large d.

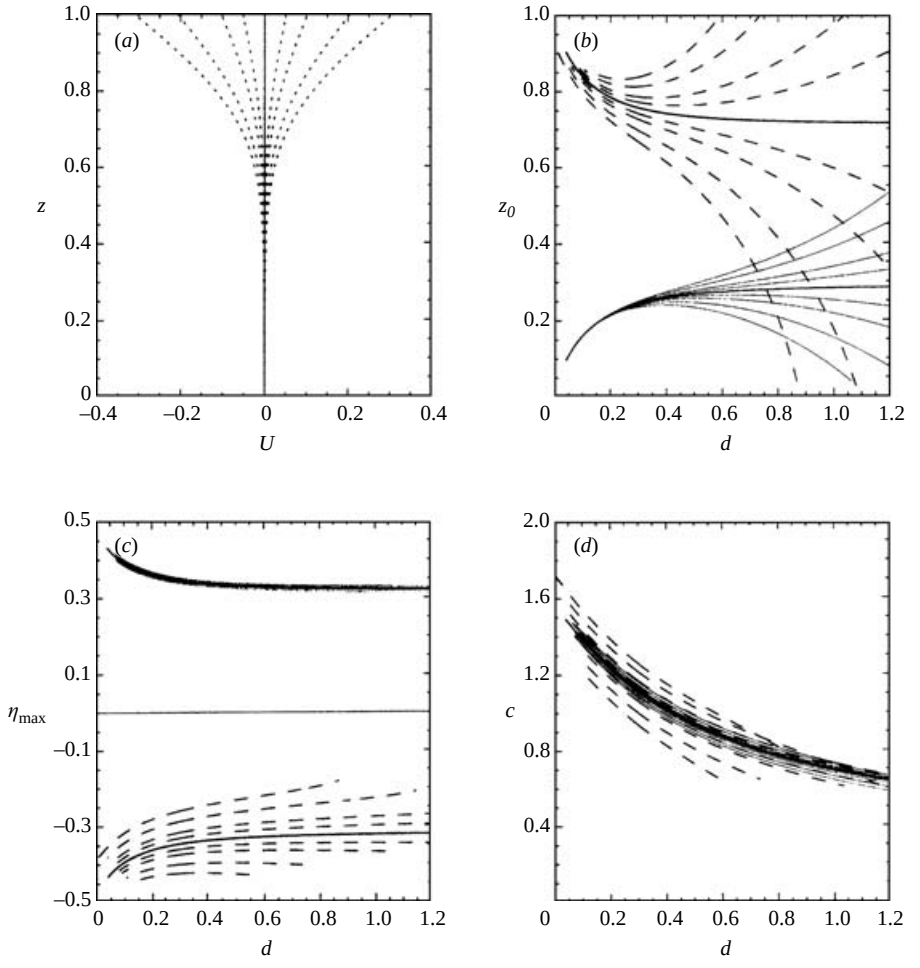

FIGURE 2. Properties of conjugate flows at the breaking limit for different background currents. (*a*) Background currents used. Parameter values are $(s_1, s_2) = (0.2, 0.75)$ and $\zeta = -1.2, -0.8, -0.4, -0.2, 0, 0.2, 0.4, 0.8, 1.2$. (*b*) Plots of $r_l(d)$ and $r_u(d)$ for the background currents shown in (*a*). Here, and in (*c*) and (*d*), the thick solid line is for the case with no background current ($\zeta = 0$), while the dashed and thin solid lines are $r_u(d)$ and $r_l(d)$ for cases with non-zero background currents. $r_u(d)$ and $r_l(d)$ both decrease as ζ increases. (*c*) Conjugate flow amplitudes at the breaking limit. Amplitudes of conjugate flows of depression (dashed lines) decrease in magnitude as ζ increases. Conjugate flows of elevation (thin solid lines) increase with ζ. (*d*) Conjugate flow propagation speed. Propagation speeds increase with ζ.

In figure 2 properties of conjugate flows at the breaking amplitude are shown for a number of background currents having different values of the vorticity parameter ζ with the other two velocity parameters held constant ($s_1 = 0.2$ and $s_2 = 0.75$). The currents are shown in panel (*a*), and the curves $r_{l,u}$ are shown in panel (*b*). In panel (*b*) the solid thick curves are for the absence of a background current, while the thin solid curves and the dashed curves are $r_l(d)$ and $r_u(d)$ respectively for non-zero ζ. Both sets of curves move down (decrease) as ζ increases. In some cases (large ζ) the curves $r_l(d)$ and $r_u(d)$ cross, indicative of the existence of waves of elevation and depression for the same stratification and background current. In figure 2(*c*) the amplitude of the conjugate flow (extreme values of η) is shown. The conjugate flows of elevation are

insensitive to the value of ζ. For these conjugate flows the centre of the pycnocline is generally below 0.5 and is below the region of non-zero U (see figure 2*b*). It should be born in mind that for d greater than about 0.3 significant stratification can extend into the vorticity layer. Waves of elevation break at the bottom of the domain where the vorticity in the background flow is negligible. In contrast, the amplitude of the conjugate flows of depression are sensitive to ζ, decreasing in magnitude as ζ increases. Waves of depression have positive wave-induced vorticity and break near the surface. As ζ increases the vorticity of the background flow increases, enhancing the vorticity in the waves and hence increasing the near-surface flow relative to c. Thus, as ζ increases, the breaking amplitude decreases. This also explains why $r_u(d)$ decreases with ζ. In figure 2*d*, the propagation speeds of the conjugate flows at the breaking limit are shown. They increase with ζ, with those for conjugate flows of depression increasing most rapidly. The large decrease of c as a function of d is in part due to the decrease in the bottom-to-surface density difference. If the propagation speeds are scaled by the square-root of $\bar{\rho}(0) - \bar{\rho}(1)$ the conjugate flow propagation speeds for $d < 0.1$ are virtually unchanged while at $d = 1.2$ they cluster around 1.04 with a larger spread. Subtracting the vertically averaged background current reduces the spread by about one half.

Similar comparisons were made for background currents with fixed ζ and s_2 for different values of s_1. For s_1 between 0.2 and 0.05 the results were not very sensitive to the value of s_1.

4. Shoaling behaviour and the formation of waves with trapped cores

In this section the results of a large number of model runs are summarized. Stratifications using four different pycnocline widths, $d = 0.05$, 01, 0.25 and 0.4, were considered with either no background current or a background current of the form (5) with velocity parameters $(\zeta, s_1, s_2) = (1.2, 0.2, 0.75)$ (see figure 2).

For cases without a background current and using pycnocline widths of 0.05, 0.1 and 0.25, a shelf amplitude $a_T = 1.5$ was used, resulting in a deep-water depth of 2.5. The shelf width was $L = 5$ and the horizontal grid spacing was $\delta x = 0.05$. The computational domain extended between -100 and 100. For all other cases a shelf amplitude $a_T = 3$ was used, resulting in a deep-water depth of 4. The shelf width was 10 and δx was normally 0.2. The horizontal resolution was tripled for some runs to verify the accuracy of the results. The computational domain extended between $x = -100$ and $x = 200$, except for stratifications with $d = 0.4$. The slower evolution of the waves, in both distance and time, for these stratifications made a longer domain necessary (see Lamb 2002). This is a consequence of a more linear stratification, which weakens the nonlinearity, and the fact that for these stratifications the pycnocline tended to be closer to the mid-depth. Thus, the shallow-water conjugate-flow amplitude tended to be smaller, further weakening the nonlinearity. For these model runs the right boundary of the computational domain was moved to $x = 400$. Even with this extended domain, waves failed to reach a final form in some cases with $U_{\max}/c < 1$. Because $U_{\max}/c$ is decreasing with time, due to a decrease in $U_{\max}$ (c remains constant), it is clear that they will not eventually form cores.

4.1. *Cases with no background current*

The results obtained without a background current are summarized in figure 3. Here, the curve $r_u(d)$ is shown along with the curves (dashed) along which the minimum Richardson number in the conjugate flow equals 0.25 and 0.5, the former

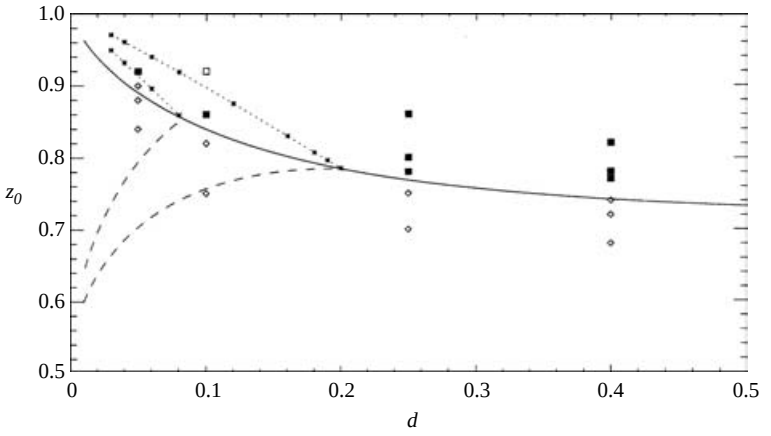

FIGURE 3. Summary of shoaling wave simulations for cases with no background current. The solid curve is $r_u(d)$. Along dashed curves the conjugate flow has a minimum Richardson number of 0.25 (left curve) and 0.5 (right curve). Along dotted curves the minimum Richardson number is 0.25 and 0.5 in the solitary wave at the breaking amplitude. For these curves the minimum Richardson number is the minimum in the stratified portion of the fluid, and is not necessarily the global minimum. Solid squares indicate stratifications for which waves with trapped cores are formed after a sufficiently large initial wave shoals into shallow water ($U_{\max}/c > 1$). Open diamonds are stratifications for which waves with trapped cores were not formed ($U_{\max}/c < 1$) regardless of the initial wave amplitude. The open square is for a stratification for which a large initial wave results in an unstable wave in shallow water which has $U_{\max}/c$ oscillating between about 1 and 1.01 but for which no closed contours can be seen in density contour plots.

having the smaller value of d. These are given for reference only. The 'minimum' value used is that in the stratified region of the water column. The minimum over the whole depth may be less, particularly for small d, in which case the fluid is very weakly stratified near the lower boundary. For values of (d, z_0) above $z = r_u(d)$, solitary waves which can be numerically computed are limited in amplitude by the breaking limit, or, for small d, by the stability limit. Below the curve $z = r_u(d)$ but above $z = r_l(d) = 1 - r_u(d)$, amplitudes are limited by the conjugate flow limit except for points close to, or below, the curve $Ri = 0.25$, in which case they are again limited by the stability limit. As the centre of the pycnocline moves towards the upper boundary, so that z_0 increases, the conjugate flow amplitude increases and the minimum Richardson number decreases. The conjugate flow amplitude is approximately $|z_0 - 0.5|$ for small value of d.

Because only shoaling waves of depression have been considered for stratifications without a turning point (i.e. $z_0 > 0.5$), the curve $r_l(d)$ is not relevant and hence is not shown in figure 3.

For a specified stratifications, with d and z_0 fixed, let $(\tilde{d}, 1 - \tilde{z}_0) = (d/D(x), (1 - z_0/D(x))$, where $D(x)$ is the local water depth. The values of $(\tilde{d}, \tilde{z}_0)$ vary with depth such that the point $(\tilde{d}, \tilde{z}_0)$ moves along a straight line, going through $(0, 1)$ in the limit $D(x) \to \infty$. Thus, figure 3 can be used to determine limiting behaviour of the initial deep-water waves. For this purpose, figure 2 also includes the curves along which the minimum Richardson number (dotted line defined as for the conjugate flow curves) in a solitary wave at the breaking amplitude is equal to 0.25 and 0.5. For fixed d and z_0, wave amplitudes are limited by the conjugate-flow limit in sufficiently shallow water provided the pycnocline remains at or above the mid-depth ($\tilde{z}_0$ close

to 0.5). As the water depth increases the limiting behaviour switches to the stability limit for large $(1-\tilde{z}_0)/\tilde{d}$, or to the breaking limit for small $(1-\tilde{z}_0)/\tilde{d}$. For the thin pycnocline cases, $d=0.5$, the initial deep-water waves were limited in size by the stability limit, which made it difficult to get waves to break as they shoaled.

The large number of model runs without a background current are also summarized in figure 3. Solid squares indicate stratifications for which sufficiently large initial waves evolved into waves with a trapped core after shoaling. These cases are all above the curve $z_0=r_u(d)$, i.e. for stratifications without a conjugate flow with open streaklines. Cases for which waves with trapped cores were not formed after shoaling, regardless of the initial wave amplitude, are indicated by the open diamonds. These cases are below or slightly above the curves $z_0=r_u(d)$. The open square indicates a special case, discussed below. Details of some of the model runs are provided in table 1. The table includes information on the initial and final waves, as well as on whether closed density contours occurred in the final wave. Values of the minimum Richardson number in the initial wave are also given. This value, as discussed above, is not necessarily the global minimum but is the minimum value in the pycnocline, and hence is due to high shear rather than low values of buoyancy frequency. For stratifications in which the maximum initial wave is limited by the stability limit, the maximum wave has a minimum Richardson number in the pycnocline of about 0.25. The propagation speed of the final wave was determined by tracking the position where the surface current was equal to 0.6.

In all cases shoaling waves steepen at the back as they shoal. If of sufficient amplitude they overturn. The question is what happens afterwards. For stratifications with wide pycnoclines ($d=0.25$ and 0.4), lying below $r_u(d)$, waves which overturned formed a patch of surf at the rear of the wave which was gradually left behind. For the large initial waves considered here, the leading waves arriving in the shallow water had an amplitude larger than the maximum possible, conjugate-flow limited, wave amplitude. They gradually adjusted towards a flat-centred wave by flattening out at the front. Over time the flat part of the wave lengthened and the much larger amplitude at the rear of the wave slowly diminished in size. Figure 4(*a*) shows an example of such an evolving wave using the stratification $(d, z_0)=(0.25, 0.7)$. As z_0 increases, the surf at the rear of the wave lasts longer and the adjustment to a final state occurs more slowly. For stratifications with z_0 above the critical curve, shoaled waves have a persistent surf at the rear of the wave. Closed density contours form; however, they are patchy and confined to the back portion of the wave for z_0 close to $r_u(d)$. They do not fill the whole wave. Shoaled waves have $U_{\max}/c>1$ for sufficiently large initial waves. As z_0 increases the closed density contours are better defined and become more persistent (e.g. figure 4*b*). Figure 4(*c*) shows the final shoaled wave for a stratification lying further above the critical curve ($(d, z_0)=(0.25, 0.86)$). The region of closed density contours fills more of the wave.

Figure 4(*d–f*) shows waves at the end of three model runs for stratifications with $d=0.4$ and $z_0=0.76$, 0.77 and 0.82, all lying above $r_u(0.4)=0.7413$. Cases with $d=0.4$ evolve more slowly than those with $d=0.25$, requiring a longer domain. Note that outside the wave core these waves are horizontally uniform, suggesting the existence of conjugate flows with trapped cores. Such waves were also reported by Lamb (2002) where for some stratifications shoaled waves with trapped cores appeared to have a limiting wave amplitude.

For a narrower pycnocline thickness $d=0.1$, for which $r_u(0.1)=0.8395$, the results were qualitatively similar. For the stratifications below the critical curve, with $z_0=0.75$ and 0.82, waves with trapped cores were not obtained. Initial wave amplitudes were

			Initial wave				Final wave		
d	z_0	a/b	$\eta_{\max}$	Ri	c	$\frac{U_{\max}}{c}$	c	$\frac{U_{\max}}{c}$	Core
0.4	0.72	b	0.640	0.79	2.08	0.92	1.02	0.94*	No
			0.717	0.66	2.15	0.97	1.02	0.92*	No
	0.77	a	0.612	0.75	1.98	0.95	1.01	1.02	Yes
			0.673	0.61	2.04	0.996	1.01	1.03	Yes
	0.82	a	0.231	4.12	1.49	0.51	0.988	0.91	No
			0.413	1.34	1.69	0.79	1.00	1.04	Yes
			0.571	0.72	1.85	0.97	1.00	1.09	Yes
0.25	0.7	b	0.412	1.01	1.85	0.79	1.18	0.80*	No
			0.556	0.64	1.97	0.88	1.18	0.86*	No
			0.690	0.48	2.06	0.97	1.19	0.90*	No
	0.75	b	0.440	0.83	1.82	0.85	1.18	0.92*	No
			0.523	0.64	1.88	0.93	1.18	0.96*	No
			0.588	0.55	1.94	0.98	1.18	0.97*	No
	0.78	a	0.504	0.63	1.83	0.96	1.18	1.003	No
			0.543	0.57	1.84	0.99	1.18	1.02	Yes
	0.8	a	0.417	0.80	1.70	0.90	1.17	1.05	Yes
			0.471	0.66	1.76	0.95	1.17	1.06	Yes
	0.86	a	0.385	0.72	1.56	0.96	1.13	1.15	Yes
0.1	0.75	b	0.482	0.38	2.07	0.79	1.40	0.69	No
			0.587	0.29	2.16	0.84	1.40	0.69	No
			0.627	0.26	2.20	0.86	1.40	0.69	No
	0.82	b	0.488	0.34	1.98	0.92	1.39	0.92	No
			0.523	0.31	2.02	0.93	1.39	0.93	No
			0.582	0.27	2.09	0.96	1.39	0.93	No
	0.86	a	0.332	0.50	1.68	0.91	1.36	0.98	No
			0.390	0.41	1.77	0.95	1.38	1.03	Yes
			0.425	0.37	1.83	0.98	1.38	1.04	Yes
	0.92	a	0.228	0.60	1.31	0.98	1.19	1.0	No
			0.236	0.57	1.33	0.99	1.20	1.01	No
0.05	0.84	b	0.196	0.64	1.59	0.62	1.40	0.65	No
			0.268	0.40	1.73	0.71	1.45	0.73	No
			0.358	0.27	1.87	0.79	1.48	0.80	No
	0.88	b	0.342	0.27	1.76	0.88	1.45	0.91	No
			0.356	0.25	1.79	0.89	1.46	0.91	No
	0.9	a	0.322	0.28	1.68	0.93	1.42	0.96	No
			0.355	0.25	1.74	0.98	1.45	0.98	No
	0.92	a	0.278	0.30	1.54	0.98	1.37	1.01	Yes

TABLE 1. Properties of the initial and final waves for cases with no background current. a/b refers to position (above or below) relative to the critical curve $r_u(d)$ (see figure 2). Core refers to the presence or non-presence of closed density contours. An asterisk beside the value of U_m/c for the final wave indicates that the shoaling wave had not reached a final form. See text for discussion.

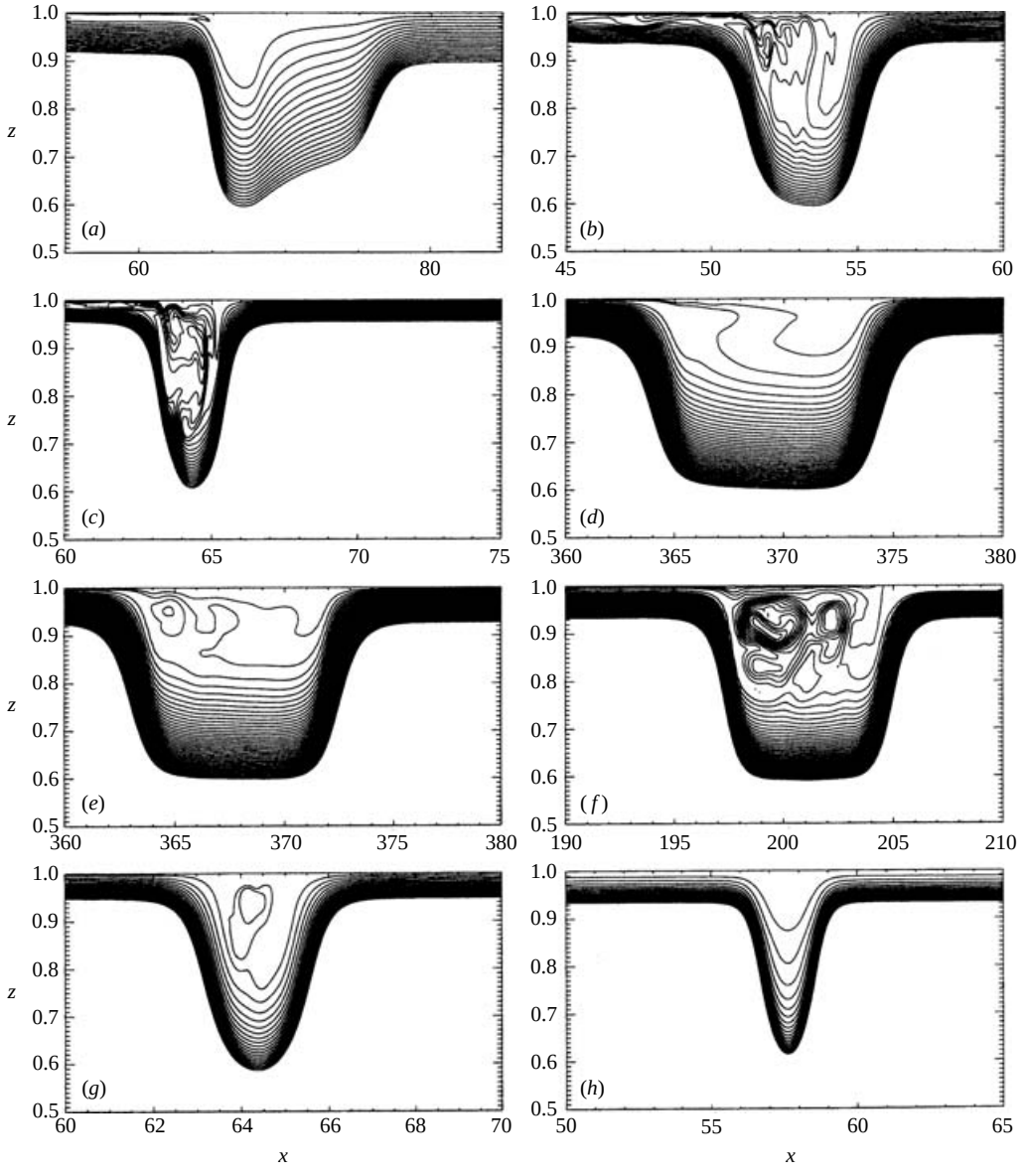

FIGURE 4. Density contour plots of the leading wave after shoaling. Only density contours for small values of ρ are shown. (*a*) $(d, z_0) = (0.25, 0.7)$, initial wave amplitude 0.690; (*b*) $(d, z_0) = (0.25, 0.8)$, initial amplitude 0.471; (*c*) $(d, z_0) = (0.25, 0.86)$, initial amplitude 0.385; (*d*) $(d, z_0) = (0.4, 0.76)$, initial amplitude 0.717; (*e*) $(d, z_0) = (0.4, 0.77)$, initial amplitude 0.612; (*f*) $(d, z_0) = (0.4, 0.82)$, initial amplitude 0.571; (*g*) $(d, z_0) = (0.1, 0.86)$, initial amplitude 0.425; (*h*) $(d, z_0) = (0.05, 0.88)$, initial amplitude 0.356.

limited by the stability limit, with minimum Richardson numbers of 0.26 and 0.27 and maximum values of $U_{\max}/c$ equal to 0.86 and 0.96 respectively. When wave breaking occurred, the patch of breaking at the rear of the wave was rapidly left behind. For a stratification above the critical curve, with $z_0 = 0.86$, waves with trapped cores were formed. An example is shown in figure 4(*g*). For a pycnocline closer to the upper boundary, with $z_0 = 0.92$, waves with permanent trapped cores are not formed. Initial

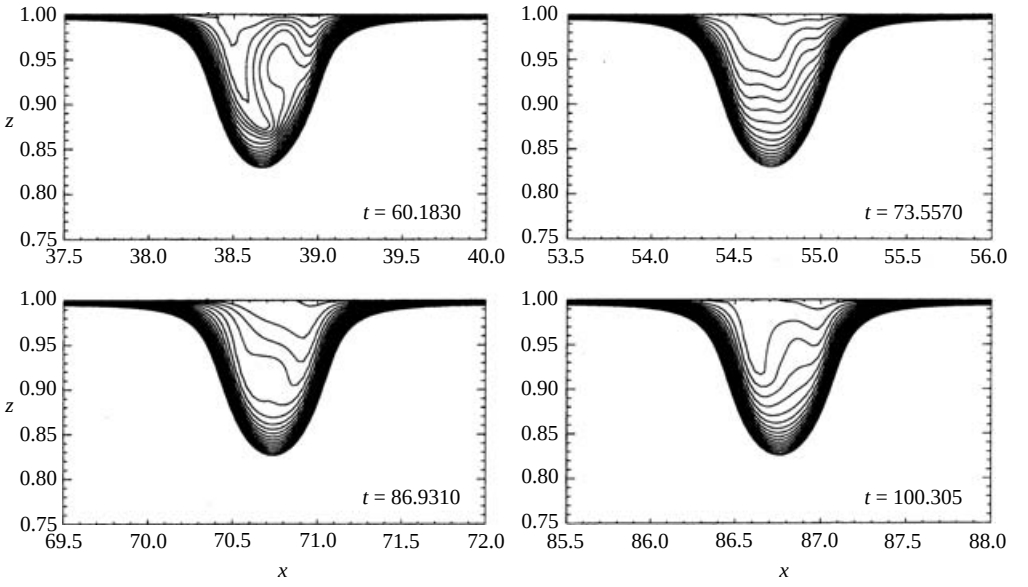

FIGURE 5. Unstable solitary wave after shoaling for stratification $(d, z_0) = (0.1, 0.92)$ and initial amplitude 0.236. As in figure 3 contours are shown for small density values only. No closed contours are seen; however $U_{\max}/c$ oscillates between 1 and 1.01 suggesting some recirculation may be occurring.

waves close to the breaking limit shoal to form what appear to be unstable waves in the shallow water. Perturbations within the solitary wave appear in the front half of the wave, grow and propagate to the rear of the wave. This cycle repeats (see figure 5). During the course of each cycle the ratio $U_{\max}/c$ varies between slightly below and slightly above 1.0. The smallest Richardson number observed in the near-surface region of the solitary wave is about 0.244, slightly below the critical value of 0.15.

Some thin stratifications, with $d = 0.05$ ($r_u(0.05) = 0.8905$) were also considered. For stratifications with $z_0 = 0.84$, wave breaking did not occur during shoaling. For stratifications with $z_0 = 0.88$ breaking occurred but no waves with trapped cores were formed. The final wave with an initial amplitude of 0.356 is shown in figure 3(*h*). For these two stratifications the largest initial waves had minimum Richardson numbers of 0.27 and 0.25 respectively and hence were close to the largest possible (the waves are bounded by the instability limit); however the initial values of $U_{\max}/c$ were 0.88 and 0.89, significantly less than 1.

Cases slightly above the critical curve with $z_0 = 0.9$ also did not form waves with trapped cores. For this value of z_0 the largest initial wave that could be computed had a minimum Richardson number of 0.25 and was close to breaking ($U_{\max}/c = 0.98$). If some way could be found to initialize the model with larger waves it is possible that shoaling waves could form waves with trapped cores. For a stratification further above the critical curve, at $z_0 = 0.92$, waves with trapped cores were formed.

4.2. *Cases with a sheared background current*

We now turn to the results obtained with a background sheared current with velocity parameters $(\zeta, s_1, s_2) = (1.2, 0.2, 0.75)$. In figure 6 the curves $r_u(d)$ and $r_l(d)$ for this background current are shown again. Also shown are the curves for minimum Richardson number in the conjugate flow equal to 0.25 and 0.5. The curves for

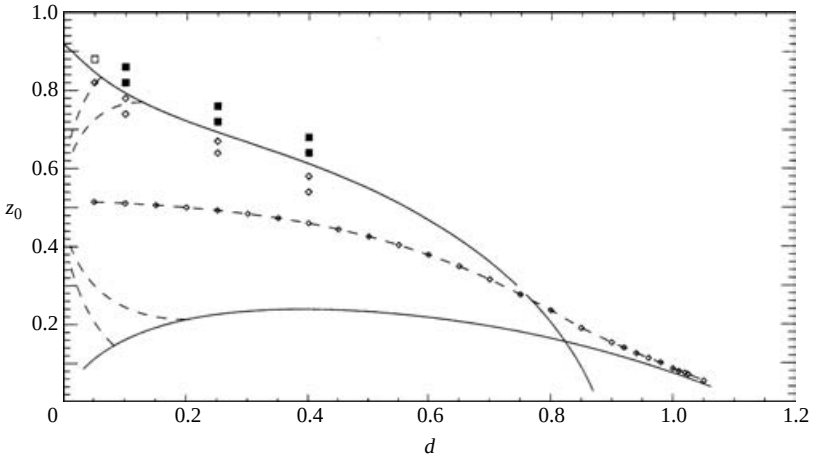

FIGURE 6. As for figure 3 but for shoaling waves in the presence of the background current $(\zeta, s_1, s_2) = (1.2, 0.2, 0.75)$. Minimum Richardson numbers in waves at breaking limit not shown. See text for explanation.

solitary waves at the breaking limit have minimum Richardson numbers equal to 0.25 are not shown because the vertical profile of the Richardson number through the centre of a solitary wave in the presence of the background sheared current does not necessarily have a local minimum in the pycnocline. The bounding curves $r_u(d)$ and $r_l(d)$ cross near $d = 0.85$, indicating the coexistence of a conjugate flow of elevation and depression. Calculation of $r_u(d)$ showed some interesting behaviour. For conjugate flows of depression the eigenvalue problem (12) is solved by specifying $\eta'(1)$ and integrating down, since for waves of depression wave breaking occurs at the surface so it was expected that $\eta'(1)$ would be close to 1 for stratifications with $z_0 = r_u(d)$. Indeed, it was equal to 1, indicating that breaking first occurs at the surface. When considering T as a function of $\eta'(1)$, one finds that there are two roots along $z_0 = r_u(d)$. For small values of d the first root is at $\eta'(1) = 1$ while the second root is for a value of $\eta'(1)$ greater than 1, giving an invalid conjugate-flow solution. As d increases the second root decreases until at a critical value d_c, slightly larger than 0.75, the two roots merge. For still larger values of d the first root is smaller than 1 while the second root is at $\eta'(1) = 1$. This is illustrated in figure 7(*a*), where T profiles are shown for three points along $r_u(d)$, namely $(d, z_0) = (0.766, 0.26545)$, (0.76, 0.27514) and (0.75, 0.29038). The first two of these sets of values are to the right of d_c, the third is to the left. These illustrate that the first root rapidly decreases as d increases. It is at $\eta'(1) = 0.6, 0.32$ and 0.18 when $d = 0.76$, 0.766 and 0.768 respectively. It no longer exists when $d = 0.77$. The small region of double roots implies the existence of a region in which two conjugate flows of depression exist simultaneously. In figure 6 the jump from the left- to the right-hand root is indicated by the break in $r_u(d)$ near $d = 0.75$.

Also shown in figure 6 is the curve $z = A_0(d)$ along which the conjugate flow amplitude is zero. This curve was obtained by starting with the conjugate-flow solutions along the curve $r_l(d)$ and then computing solutions for gradually increasing values of z_0 until the amplitude became extremely small. The values at which the conjugate flow amplitude is equal to zero were then obtained via extrapolation. For $d < d_c$, decreasing z_0 from $z_0 = r_u(d)$ until the conjugate flow amplitude goes to zero results in the same value of z_0. For $d > d_c$, moving off the curve $r_u(d)$ soon results in

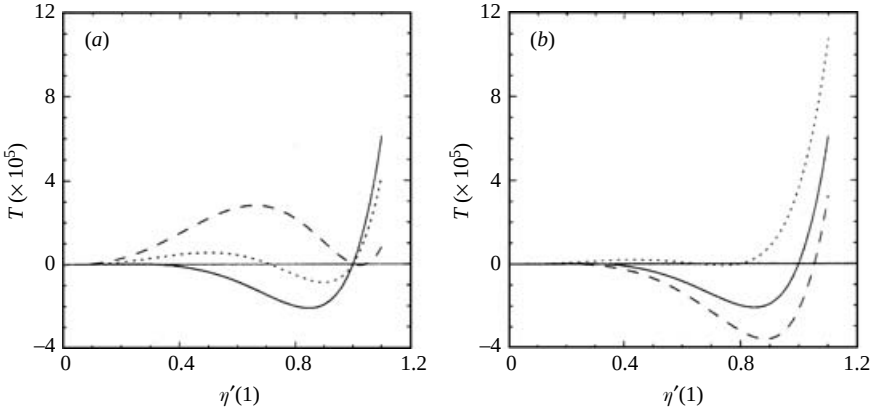

FIGURE 7. Profiles of $T(\eta'(1))$ for stratifications with a background current. (*a*) Profiles for three stratifications along $z_0 = r_u(d)$: $(d, z_0) = (0.766, 0.26545)$ (solid), $(0.76, 0.27514)$ (dotted) and $(0.75, 0.29038)$ (dashed). (*b*) Profiles for three stratifications with $d = 0.766$. Curves are for $z_0 = r_u(0.766) = 0.26545$ (solid), 0.2645 (dashed) and 0.267 (dotted).

the disappearance of solutions. This is illustrated in figure 7(*b*) where three profiles of T are shown for three different values of z_0 using $d = 0.766$. The solid curve, for $z_0 = r_u(0.766) = 0.26545$, passes through $T = 0$ at $\eta'(1) = 1$. When z_0 is decreased slightly to 0.2645 (dashed curve) the first root is at 0.2 while the second is greater than 1. When z_0 is increased slightly to 0.267 the two roots are at $\eta'(1) = 0.65$ and 0.8 (dotted curve). They disappear at about 0.2671. In particular, the second of the two roots does not go to zero as z_0 increases, as would be the case if the amplitude of the conjugate flow solutions went to zero.

Note that unlike for figure 3, the use of a fixed background current to generate figure 6 means that the figure cannot be used to deduce anything about limiting wave amplitudes for the initial deep-water waves.

Figure 6 also summarizes the results of a large number of model runs of shoaling solitary waves in the presence of a background current. As in figure 3 solid squares indicated stratifications for which sufficiently large initial waves formed a core after shoaling. Open diamonds indicate stratifications for which shoaling waves did not form cores regardless of the initial wave amplitude. The open square is again for a stratification for shoaled waves with $U_{\max}/c > 1$, no closed density contours, and appears to be unstable like the one depicted in figure 5. As for shoaling waves in the absence of a background current, waves with cores were only formed in stratifications with $z_0 > r_u(d)$. Details of some of the model runs are provided in table 2. Minimum Richardson numbers are not included as there often was no local minimum in the pycnocline and hence the minima occurred at the lower boundary and were very small.

The qualitative behaviour of the shoaling waves is similar to that for cases without a background current and so are not discussed in detail. Note that the peak near-surface background current is approximately 10–30% of the propagation speed of the waves in shallow water (see table 2).

5. Summary

The presence of a background sheared current can significantly modify the properties of large-amplitude solitary waves. In particular, a surface sheared layer can

			Initial wave			Final wave		
d	z_0	a/b	$\eta_{\max}$	c	$\frac{U_{\max}}{c}$	c	$\frac{U_{\max}}{c}$	Core
0.4	0.54	b	0.525	2.375	0.88	1.13	0.94*	No
			0.616	2.456	0.96	1.13	0.95*	No
	0.58	b	0.488	2.299	0.88	1.14	0.97*	No
			0.517	2.327	0.91	1.14	0.97*	No
			0.593	2.399	0.98	1.14	0.97*	No
			0.636	2.438	1.01	1.14	0.97*	No
	0.64	a	0.366	2.099	0.80	1.15	1.02	Yes
			0.532	2.278	0.98	1.16	1.02	Yes
	0.68	a	0.177	1.823	0.55	1.15	0.96	No
			0.264	1.928	0.69	1.17	1.01	No
			0.330	2.005	0.79	1.17	1.04	Yes
			0.429	2.119	0.91	1.17	1.06	Yes
			0.506	2.203	0.99	1.17	1.07	Yes
0.25	0.64	b	0.551	2.441	0.96	1.31	0.92*	No
			0.598	2.490	0.99	1.31	0.91*	No
–	0.67	b	0.451	2.288	0.91	1.32	0.95*	No
			0.568	2.424	1.004	1.32	0.95*	No
	0.72	a	0.396	2.147	0.92	1.33	1.03	Yes
			0.478	2.253	0.99	1.33	1.04	Yes
	0.76	a	0.300	1.946	0.85	1.33	1.006	No
			0.366	2.041	0.94	1.33	1.03	Yes
			0.419	2.115	0.99	1.33	1.08	Yes
0.1	0.74	b	0.419	2.343	0.88	1.53	0.85	No
			0.484	2.432	0.92	1.53	0.85	No
			0.562	2.531	0.96	1.53	0.85	No
			0.606	2.583	0.98	1.53	0.85	No
	0.78	b	0.401	2.255	0.92	1.54	0.95	No
			0.458	2.341	0.96	1.54	0.95	No
			0.506	2.409	0.99	1.54	0.96	No
	0.82	a	0.376	2.146	0.97	1.55	1.002	Yes
			0.406	2.195	0.99	1.55	1.02	Yes
			0.424	2.224	1.006	1.55	1.03	Yes
	0.86	a	0.200	1.722	0.86	1.46	0.97	No
			0.252	1.833	0.94	1.49	1.02	Yes
0.05	0.82	b	0.405	2.26	0.91	1.62	0.92	No
	0.88	a	0.335	2.054	0.98	1.63	1.09	No

TABLE 2. Properties of the initial and final waves for cases with a background current $(\zeta, s_1, s_2) = (1.2, 0.2, 0.75)$. a/b refers to position (above or below) relative to the critical curve $r_u(d)$ (see figure 5). Core refers to the presence or non-presence of closed density contours. An asterisk beside the value of U_m/c for the final wave indicates that the shoaling wave had not reached a final form. See text for discussion.

have a pronounced effect on waves of depression, changing solitary internal waves of depression with open streaklines from being conjugate-flow limited to being breaking limited if the near-surface vorticity of the background current has the same sign as that induced by the wave. Furthermore, numerical evidence has been presented which suggests that, at least for several stratifications from the important family of stratifications with a single hyperbolic tangent pycnocline, the limiting behaviour of waves with open streaklines determines whether or not waves with trapped cores can be formed as waves shoal from deep to shallow water. Cases with no background current and a background current with non-zero shear in the upper 25% of the water column were considered. It was found that if waves in the shallow water have a conjugate flow with open streaklines then shoaling waves will not form waves with trapped cores. On the other hand, if waves with open streaklines are limited in amplitude by the breaking limit in the shallow water, as large deep-water waves shoal they form waves with a persistent surf at the back of the wave, if waves are close to having a conjugate flow with open streaklines, or waves with a well-defined trapped cores.

Two critical curves, given by $z_0 = r_l(d)$ and $z_0 = r_u(d)$ were z_0 is the centre of the pycnocline and d is the pycnocline width parameter (see (4)), were found along which conjugate flows of elevation and of depression, respectively, are at the breaking limit. As the background shear ζ increases (see (5)), both $r_l(d)$ and $r_u(d)$ decrease. For sufficiently large values of ζ they cross, suggesting the existence of solitary waves of elevation and of depression for the same stratification (this was not investigated). The largest sheared current considered, with $\zeta = 1.2$, was investigated in more depth and was used for the shoaling wave simulations. It had a maximum current of about 0.3 at the surface, approximately 20–30% of the propagation speed of the shoaled waves. It was found that at a critical value of the width parameter, d_c, less than that at which $r_l(d) = r_u(d)$, the character of the conjugate flows of depression changes. When $d < d_c$, as z_0 decreases the conjugate flow amplitude decreases monotonically to zero at $z_0 = A_0(d)$ and there is only one conjugate flow of depression. When $d > d_c$ there are two conjugate flows of depression and, as z_0 increases, the conjugate flow solution which is at the breaking amplitude when $z_0 = r_u(d_c)$ decreases in amplitude but disappears before the conjugate flow amplitude goes to zero.

For the shoaling wave simulations attention was focused on values of d much less than d_c ($d_c \approx 0.75$ in background current, giving a nearly linear stratification). In this case solitary waves in the shallow water are waves of depression provided $z_0 > A_0(d)$. Only such cases were considered. Solitary waves of depression with open streaklines are limited by the conjugate flow limit if $z_0 < r_u(d)$ and by the breaking limit if $z_0 > r_u(d)$, except for very small values of d in which case they are limited by the instability limit. All waves steepen at the back as they shoal. For stratifications with z_0 well below $r_u(d)$, sufficiently large initial waves break at the back as they shoal. The resulting surf is rapidly left behind. As z_0 increases the surf lasts longer and as z_0 becomes slightly larger than $r_u(d)$ a solitary wave in shallow water is formed that has a permanent surf, with closed density contours, in the rear portion of the wave. As z_0 increases still further the region of closed density contours fills more of the wave until eventually the shoaled wave with a trapped core is almost symmetric about the centre of the wave.

Although dissipation and mixing were not considered, these results give some insight into dissipation processes associated with shoaling solitary waves. For stratifications for which conjugate flows far from the breaking amplitude exist in shallow water, the surf associated with overturning waves is rapidly left behind. As the conjugate

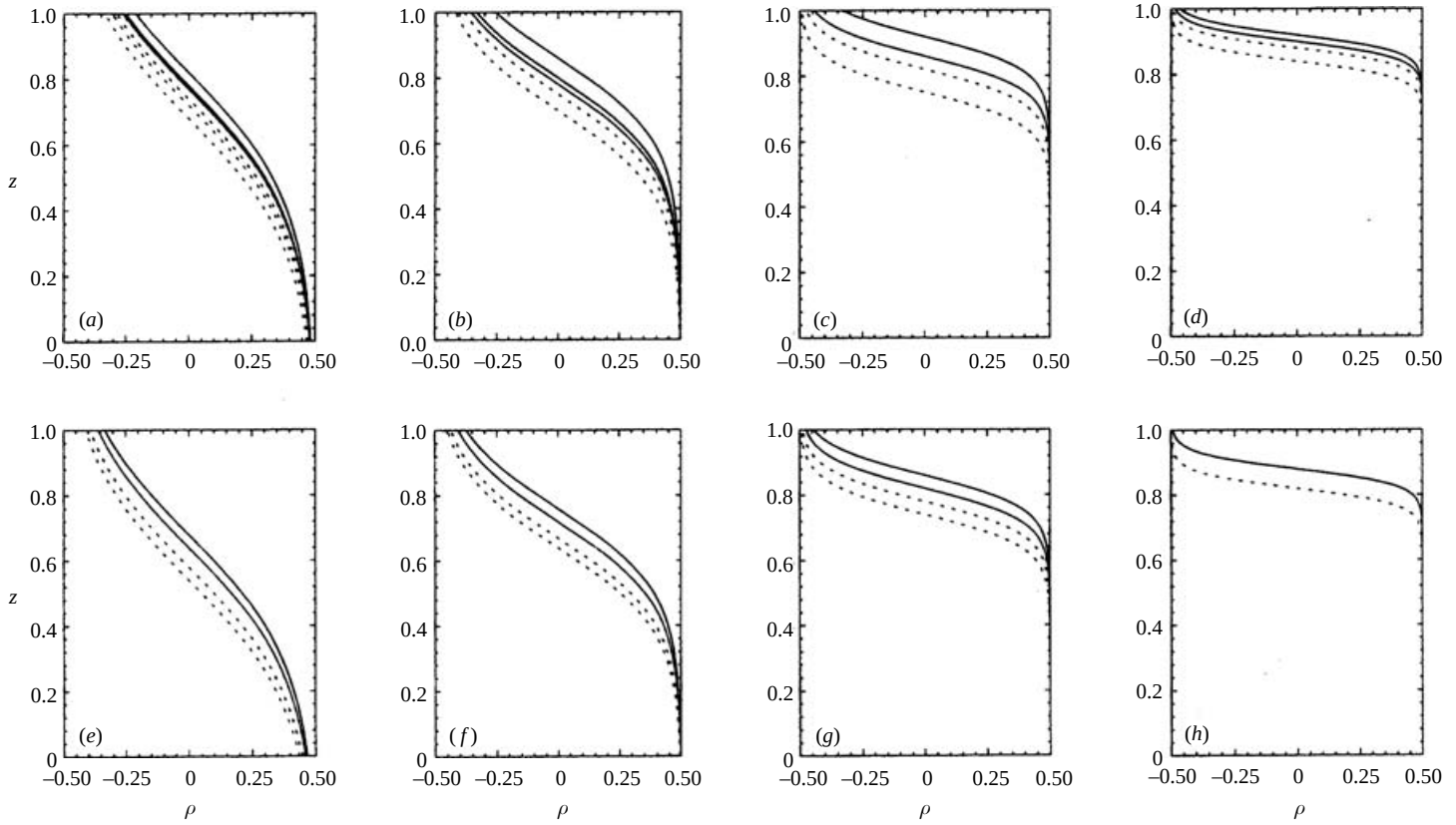

FIGURE 8. Density profiles used for the model simulations. Solid(dotted) curves are stratifications for which waves with trapped cores could(could not) be formed via shoaling. (*a–d*) No background current, $d = 0.4$, 0.25, 0.1 and 0.05, respectively. (*e–h*) With background current $(\zeta, s_1, s_2) = (1.2, 0.2, 0.75)$, $d = 0.4$, 0.25, 0.1 and 0.05, respectively.

flows approach and pass the breaking amplitude the surf persists for longer times and distances. This has implications for the distribution of mixing associated with shoaling internal waves at the shelf break. An investigation of the energy dissipation and mixing associated with shoaling waves will be the subject of future work.

In the absence of a background current, waves with trapped cores are formed only when there is significant stratification at the surface. Because a surface mixed layer is normally present, waves will usually be conjugate-flow limited with the result that mixing will occur near the region of depth change. The presence of a background current, with near-surface shear and wave-induced shear of the same sign, makes waves with trapped cores possible in stratifications which could otherwise not support such waves. Figure 8 shows all the stratifications considered. Solid lines show cases for which shoaling waves with trapped cores were formed. Dotted lines show stratifications for which waves with trapped cores were not formed. The effect of a background current increases as the pycnocline becomes thicker. This is perhaps not surprising as wider pycnoclines can be moved further down for the same reduction in stratification at the upper boundary.

Typical ocean stratifications are perhaps more likely to support mode-2 waves with trapped cores. Such waves are easily generated in the laboratory (e.g. Davis & Acrivos 1967); however to the author's knowledge no observations of such waves have been made in the ocean. The role of such waves in the ocean warrants future investigation.

One model run was made with a double shelf using the stratification $(d, z_0) = (0.25, 0.7)$ and no background current. The deep-water depth was 5. The water depth decreased to 2.5 where it was held constant before then decreasing to the final deep water depth of 1. In the shallow water ISWs are conjugate-flow limited (see figure 3). In the intermediate region $(\tilde{d}, \tilde{z}_0) = (0.1, 0.88)$ and from figure 3 it can be seen that ISWs are limited by the breaking limit. A deep-water wave with an initial amplitude of 0.85 and with $U_{\max}/c = 0.98$ shoaled to the intermediate depth where a wave with a trapped core was formed. After shoaling to the shallow-water depth the trapped core disappeared as the wave evolved to one with a flat centre with $U_{\max}/c < 1$.

The numerical calculation of conjugate flows for a specified stratification and background current is computationally very cheap and provides a simple means to determine whether waves with trapped cores can exist.

This work was funded by a grant from the Natural Sciences and Engineering Research Council of Canada.

REFERENCES

Amick, C. J. & Turner, R. E. L. 1986 A global theory of internal solitary waves in two-fluid systems. *Trans. Am. Math. Soc.* **298**, 431–484.

Benjamin, T. B. 1966 Internal waves of finite amplitude and permanent form. *J. Fluid Mech.* **25**, 241–270.

Brown, D. J. & Christie, D. R. 1998 Fully nonlinear solitary waves in continuously stratified incompressible Boussinesq fluids. *Phys. Fluids* **10**, 2569–2586.

Davis, R. E. & Acrivos, A. 1967 Solitary internal waves in deep water. *J. Fluid Mech.* **29**, 593–607.

Grue, F., Friis, A., Palm, S. & Rusås, P.-O. 1997 A method for computing unsteady fully nonlinear interfacial waves. *J. Fluid Mech.* **351**, 223–252.

Grue, F., Jensen, A., Rusås, P.-O. & Sveen, J. K. 1999 Properties of large amplitude internal waves. *J. Fluid Mech.* **380**, 257–278.

Grue, F., Jensen, A., Rusås, P.-O. & Sveen, J. K. 2000 Breaking and broadening of internal solitary waves. *J. Fluid Mech.* **413**, 181–217.

Holyer, J. Y. 1979 Large amplitude progressive interfacial waves. *J. Fluid Mech.* **93**, 433–448.

Lamb, K. G. 1994 Numerical experiments of internal wave generation by strong tidal flow across a finite amplitude bank edge. *J. Geophys. Res.* **99**, 843–864.

Lamb, K. G. 2000 Conjugate flows for a three-layer fluid. *Phys. Fluids* **12**, 2169–2185.

Lamb, K. G. 2002 A numerical investigation of solitary internal waves with trapped cores formed via shoaling. *J. Fluid Mech.* **451**, 109–144.

Lamb, K. G. & Wan, B. 1998 Conjugate flows and flat solitary waves for a continuously stratified fluid. *Phys. Fluids* **10**, 2061–2079.

Mehrotra, S. C. & Kelly, R. E. 1973 On the question of non-uniqueness of internal hydraulic jumps and drops in a two-fluid system. *Tellus* **25**, 560–567.

Melville, W. K. & Helfrich, K. R. 1987 Transcritical two-layer flow over topography. *J. Fluid Mech.* **178**, 31–52.

Saffman, P. G. & Yuen, H. C. 1982 Finite-amplitude innterfacial waves in the presence of a current. *J. Fluid Mech.* **123**, 459–476.

Stastna, M. & Lamb, K. G. 2002 Large fully nonlinear internal solitary waves: the effect of background current. *Phys. Fluids* **14**, 2897–2999.

Tung, K.-K., Chan, T. F. & Kubota, T. 1982 Large amplitude internal waves of permanent form. *Stud. Appl. Maths* **66**, 1–44.

Turkington, B., Eydeland, A. & Wang, S. 1991 A computational method for solitary internal waves in a continuously stratified fluid. *Stud. Appl. Maths* **85**, 93–127.

Turner, R. E. L. & Vanden-Broeck, J.-M. 1986 The limiting configuration of interfacial gravity waves. *Phys. Fluids* **29**, 372–375.

Turner, R. E. L. & Vanden-Broeck, J.-M. 1988 Broadening of interfacial solitary waves. *Phys. Fluids* **31**, 2486–2490.